Adaptive Observer for Nonlinearly Parameterised Hammerstein System with Sensor Delay – Applied to Ship Emissions Reduction

Nielsen, Kræn V.; Blanke, Mogens; Eriksson, Lars

Published in:
IEEE Transactions on Control Systems Technology

Link to article, DOI:
10.1109/TCST.2017.2715004

Publication date:
2018

Document Version
Peer reviewed version

Adaptive Observer for Nonlinearly Parameterised Hammerstein System with Sensor Delay - Applied to Ship Emissions Reduction

Kræn V. Nielsen, Mogens Blanke and Lars Eriksson

***Abstract*—Taking offspring in a problem of ship emission reduction by exhaust gas recirculation control for large diesel engines, an underlying generic estimation challenge is formulated as a problem of joint state and parameter estimation for a class of multiple-input single-output Hammerstein systems with first order dynamics, sensor delay and a bounded time-varying parameter in the nonlinear part. The paper suggests a novel scheme for this estimation problem that guarantees exponential convergence to an interval that depends on the sensitivity of the system. The system is allowed to be nonlinear parameterized and time dependent, which are characteristics of the industrial problem we study. The approach requires the input nonlinearity to be a sector nonlinearity in the time-varying parameter. Salient features of the approach include simplicity of design and implementation. The efficacy of the adaptive observer is shown on simulated cases, on tests with a large diesel engine on test bed and on tests with a container vessel.**

***Index Terms*—Nonlinear control systems, joint state and parameter observer, sensor delay.**

I. Introduction

THIS paper considers observer design for a class of systems where a bounded time-varying parameter enters the model nonlinearly. The motivation for this problem is a case of emission reduction for large diesel engines, where accurate estimation of gas composition in the scavenging air path of the engine is essential. The dynamics of this problem are described by a nonlinear model that is nonlinearly parameterized, time-varying and includes sensor delay. Literature mainly deals with systems of two kinds: are linear in the unknown parameters; have contributions from time dependent inputs and unknown parameters that enter in a simple affine manner in the system equations. The emission control problem at hand does not belong to either of these categories but is a nonlinear parameterized Hammerstein system with time-varying elements. The paper suggests a parameter and state estimation solution for this problem.

An overview of nonlinear observer design methods was presented by [1] who also defined a terminology to distinguish between adaptive observers and joint state and parameter observers. An early approach for joint state and parameter observer design for nonlinear systems was to apply an Extended Kalman Filter augmenting the state vector by the unknown parameters. This approach has problems with divergence and bias as shown in [2], who also suggested a solution for linear systems. Extension to a class of nonlinear systems was done in [3], but still for problems that were linear in the parameters. Gradient based estimators for affine systems were treated in numerous articles and in textbooks, including [4]. For nonlinearly parameterized systems, [5] showed that the gradient methods are insufficient and can lead to divergence in observers, and a min-max problem design was introduced to ensure global stability. In the present paper a guarantee of exponential convergence is essential to ensure robustness of the estimator candidates as the method is to be rolled out on a large industrial scale.

Nonlinearly parameterized perturbations were studied for a large class of nonlinear systems in [6], who also presented a stepwise design. This method was combined with a high-gain observer in [7] to generalise the design to output feedback. [8] used an observer design framework known as *Immersion & Invariance* for nonlinearly parameterised systems, under a monotonicity constraint, by adding nonlinear dynamic scaling, the purpose of which was to avoid solving partial differential equations. An uncertainty-set-based algorithm for parameter estimation was presented in [9]. This algorithm included estimates of the parameters and of the maximal set of feasible parameters. In case of nonconvex problems, the algorithm was shown capable of detecting if a local minimum was reached instead of a global one. This and most other results in literature apply to systems that fulfill some convexity or monotonicity requirements. [10] overcame this by combining traditional observer design with explorative search for part of the parameter vector. Yet another extension was presented in [11] who used virtual update laws in the design of observers where the parameter estimates include direct terms from the measurements. This facilitated implementation of update laws that are dependent on time derivatives of measurements without explicitly calculating the derivatives. Off-line estimation for multiple-input single-output (MISO) Hammerstein models were treated in [12] where the suggested approach was shown to be superior to linear methods for a chemical distillation process and a heat exchanger. The iterative approach of [13] was used for estimating the parameters of both the nonlinear and the linear parts. A recursive identification method was analyzed by [14]. A state observer for an extended Hammer-

K. V. Nielsen is with MAN Diesel & Turbo, Teglholmsgade 41, Copenhagen, Denmark and the Automation and Control Group, Dept. of Electrical Engineering, Technical University of Denmark, Kgs. Lyngby Denmark.

M. Blanke is with the Automation and Control Group, Dept. of Electrical Engineering, Technical University of Denmark, Kgs. Lyngby, Denmark and AMOS CoE, Institute of Technical Cybernetics, Norwegian University of Science and Technology, Trondheim, Norway.

L. Eriksson is with Vehicular Systems, Dept. of Electrical Engineering, Linköping University, Linköping, Sweden.

stein model of an engine test bench was presented by [15]. Parameter estimation of Hammerstein systems was treated in e.g. [16] and [17] but also these works addressed off-line identification rather than real-time estimation. In contrast, [18] presented adaptive control and real-time parameter estimation for a certain class of Hammerstein systems where the nonlinear part is linear in the unknown parameters.

This text first motivates the industrial estimation challenge from which a generic model and an estimation problem is formulated. The paper then presents both *a parameter estimator* and *a joint state and parameter observer* design for MISO Hammerstein models with first order dynamics and sensor delay. An adaptive observer is suggested that estimates the state and a time-varying parameter of the nonlinear part. Explicit calculation of derivatives is avoided by using virtual update laws inspired by [11]. Exponential convergence bounds and minimum convergence rates[1] are derived for the observer errors. The parameter error converges at least exponentially to the bounds of the time-varying parameter. A benefit of the suggested observer is shown to be the simplicity of design, of implementation and of tuning. Formal proofs for convergence and error bounds are included in the paper on conditions of fairly weak requirements on the nonlinear part of the Hammerstein model. Whereas an analytical analysis on the effect of disturbances has not been performed, the application to a real world problem demonstrates the performance of the method.

The paper first introduces the industrial case of marine emission reduction by exhaust gas recirculation in Section II and generalizes the underlying oxygen estimation problem to be one of estimating state and parameter in a nonlinear parameterized first order MISO Hammerstein system with sensor delay. An adaptive observer solution is then suggested in Section IV along with derivation of bounds and minimum convergence rates for the observer errors. The design is favorably compared to an existing but far more complex design from [7] in Section V and a simulation example follows in Section VI. The suggested observer is then applied to a high fidelity simulation of a large marine diesel engine, and to data from marine prime mover diesels on a test bed and at sea. The results show that the suggested approach is solid and yet simple to implement and therefore has the potential to become enabling technology in estimation based control of emissions from large two-stroke diesel engines.

II. The Oxygen Estimation Problem in Emission Control

Increased environmental concern has lead the International Maritime Organization to restrict the emissions from marine diesel engines [20]. The Tier III standard, that applies to vessels built after 1st of January 2016, severely restricts NO_x emission in specified NO_x Emission Control Areas (NECAs). The North American coastal area is such a NECA and the North Sea and Baltic Sea are expected to become NECAs [21]. The Tier III standard specifies a reduction by a factor of four compared to the Tier II standard, thus requiring significant modifications to the engines.

[1]Definition 5.10 in [19].

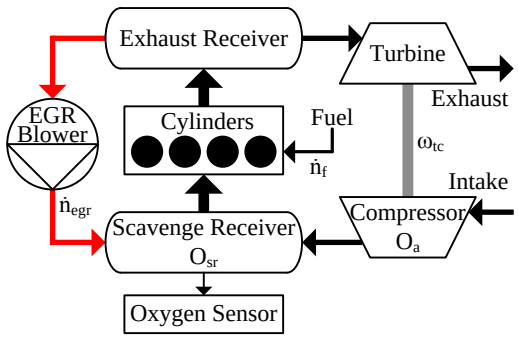

Fig. 1. Airflow of turbocharged diesel engine with high-pressure Exhaust Gas Recirculation (shown in red).

NO_x formation in a diesel engine mainly occurs during combustion where high temperatures lead to reactions between nitrogen and oxygen, known as the Zeldovich mechanism [22]. One method of decreasing NO_x formation is to install an Exhaust Gas Recirculation (EGR) system to increase heat capacity and decrease oxygen availability in the combustion. The result is lower peak combustion temperatures and thus less NO_x formation. A simplified overview of the airflow of a high pressure EGR system is shown in Figure 1. The speed of the EGR blower is used to regulate the amount of low oxygen exhaust gas that is recirculated to the scavenge receiver. Fixed gain feedback control is used to reach a setpoint for scavenge receiver oxygen fraction (O_{sr}). The pressure, temperature and gas composition of the scavenge receiver necessitates a gas extraction system in order to reliably measure O_{sr}. The gas extraction results in a measurement delay of about 20 seconds. In steady running conditions the feedback controller performs adequately in spite of this delay but in some engine loading transients O_{sr} drops excessively and the lack of oxygen causes formation of thick black smoke for more than half a minute. This is not acceptable as excessive soot formation might damage the engine and since loading transients frequently occur during maneuvering close to ports where visible smoke is restricted.

As EGR systems have only recently been added to marine two-strokes, most literature in EGR control applies to four-stroke automotive engines, where EGR is often accompanied by a variable-geometry turbocharger. High-fidelity modeling of such a system was treated in [23] and controller design in [24], [25], [26] and recently [27]. Reduction of smoke in loading transients on marine diesel engine by sophisticated control of a variable-geometry turbocharger was seen [28] but this system lacked exhaust gas recirculation. Modeling and observer design for intake manifold oxygen fraction of a diesel engine with EGR was treated in [29] where a Luenberger-like adaptive observer also estimated the fuel blend level.

High fidelity simulation models of the airflow of a marine engine with high pressure EGR were presented in [30], [31] and [32]. SISO control methods for a linearized version of such a model were investigated in [33] where it was found difficult to achieve both performance and robustness. The high-fidelity

model from [32] is used in Section VII for validation of the observer. A simpler, control-oriented model (COM) of O_{sr} was also proposed in [34] and [32] where it was shown to represent the most essential dynamics. The COM is a first order Hammerstein model (1) with molar fuel flow $\dot{n}_f$, molar EGR flow $\dot{n}_{egr}$ and turbocharger speed ω_{tc} as inputs.

$$\tau\dot{O}_{sr} = -O_{sr}+O_a-\frac{(1+\frac{y}{4}(O_a+1))\dot{n}_f\dot{n}_{egr}}{(\theta\beta(\omega_{tc})+\frac{y}{4}\dot{n}_f)(\theta\beta(\omega_{tc})+\dot{n}_{egr})} \quad (1)$$

The model includes ambient oxygen fraction O_a, ratio of hydrogen to carbon in the fuel y and a mixing time constant τ as parameters. The product $\theta\beta(\omega_{tc})$ represents the compressor flow where

$$\beta(\omega_{tc}) = (1-\phi)\frac{\omega_{tc}}{1000 \text{ rad/s}} + \phi\left(\frac{\omega_{tc}}{1000 \text{ rad/s}}\right)^2 \quad (2)$$

and ϕ is a constant. As the compressor flow model is empirical and represents a substantial simplification of the physics involved in the process, the parameter θ is expected to vary slightly depending on operating region and conditions but stay within an interval ($\theta(t) \in [\bar{\theta}-\kappa;\bar{\theta}+\kappa]$). The parameters $\bar{\theta}$ and κ depend on the engine layout and are not necessarily known a priori.

The delay of the gas extraction system (Δt) is included in the model as

$$O_{srm}(t) = O_{sr}(t-\Delta t) \quad (3)$$

where O_{srm} is the measured scavenge oxygen fraction available to the controller.

A nonlinear parameter estimator of θ for the COM was proposed in [34] but it did not consider the sensor delay, time-variance of θ and convergence bounds were not found. An observer for O_{sr} is desired in order to compensate for the delay, which impedes the EGR controller during engine loading transients.

III. A Generic System Model

The observer design proposed in this paper applies to MISO Hammerstein systems with sensor delay of the following form

$$\tau\dot{x}(t) = g(\theta(t),u(t)) - x(t) \quad (4a)$$

$$y(t) = x(t-\Delta t) \quad (4b)$$

$$\bar{\theta}-\kappa \le \theta(t) \le \bar{\theta}+\kappa \quad (4c)$$

where $x \in D_x$ is a system state within $D_x \subset R$, $u : [0,\infty) \to D_u$ is a vector of known signals within $D_u \subset R^p$, $g : D_\theta \times D_u \to D_x$ is referred to as the input nonlinearity, τ is a known positive time constant and Δt is a known time delay of the measurement $y \in D_x$. $g(\theta(t),u(t))$ is assumed to be piecewise continuous in t. The time dependency of signals is explicitly expressed when needed.

$\theta(t)$ is a time-varying parameter bounded within an interval $\theta(t) \in [\bar{\theta}-\kappa;\bar{\theta}+\kappa]$, $\kappa \ge 0$. $\bar{\theta}$ defines the middle of the interval and κ is the possible deviation from $\bar{\theta}$. It is not necessary to know the parameters $\bar{\theta}$ and κ. Theorem 1 shows that the parameter estimate of the proposed observer will converge to the interval $[\bar{\theta}-\kappa;\bar{\theta}+\kappa]$.

The input nonlinearity is required to satisfy a sector condition with respect to the parameter estimate error. With estimation errors denoted as $\tilde{x} = \hat{x} - x$, $\tilde{\theta} = \hat{\theta} - \theta$ and $\tilde{g}(\theta,\tilde{\theta},u) = g(\theta+\tilde{\theta},u) - g(\theta,u)$, the condition can be stated as

Property 1: Sector Nonlinearity
The function $\tilde{g}(\theta,\tilde{\theta},u)$ is a sector nonlinearity in $\tilde{\theta}$:

$$\forall\tilde{\theta},\exists\rho,\exists\gamma>0 : \gamma\tilde{\theta}^2 \le \tilde{g}(\theta,\tilde{\theta},u)\tilde{\theta} \le \rho\tilde{\theta}^2.$$

It can be inferred from Property 1 that $\tilde{g}(\theta,\tilde{\theta},u)$ is monotonically increasing in $\tilde{\theta}$. If g is continuously differentiable this property is satisfied if $\frac{\partial g}{\partial\theta}$ has positive bounds.

IV. Estimator design

Definition 1: A parameter estimator for the system defined by (4) is

$$\hat{\theta}(t) = k\cdot\left(\tau y(t) + \int_0^t y(t) - g(\hat{\theta}(t),u(t-\Delta t))\,\mathrm{dt}\right) \quad (5)$$

where $k > 0$.

Theorem 1: Let the estimator defined by (5) be used for estimating the time-varying parameter $\theta(t)$ of the system defined by (4). If Property 1 is fulfilled, then $\tilde{\theta}(t)$ is bounded by the relation

$$|\hat{\theta}(t)-\bar{\theta}| \le \kappa + \left(|\hat{\theta}(0)-\bar{\theta}|-\kappa\right)e^{-k\gamma t} \quad (6)$$

Proof of Theorem 1: Differentiating (5) with respect to time

$$\dot{\hat{\theta}}(t) = k\cdot\left(\tau\dot{y}(t) + y(t) - g(\hat{\theta}(t),u(t-\Delta t))\right) \quad (7)$$

Using (4b) we get

$$\dot{\hat{\theta}}(t) = k\cdot\left(\tau\dot{x}(t-\Delta t) + x(t-\Delta t) - g(\hat{\theta}(t),u(t-\Delta t))\right) \quad (8)$$

From (4a), $\tau\dot{x}(t-\Delta t)+x(t-\Delta t) = g(\theta(t-\Delta t),u(t-\Delta t))$, hence

$$\begin{aligned}\dot{\hat{\theta}}(t) &= k\cdot\left(g(\theta(t-\Delta t),u(t-\Delta t)) - g(\hat{\theta}(t),u(t-\Delta t))\right)\\ &= -k\tilde{g}(\theta(t-\Delta t),\hat{\theta}(t)-\theta(t-\Delta t),u(t-\Delta t)) \quad (9)\end{aligned}$$

The proof now splits into three cases, depending on the size of $\hat{\theta}$.

i) As a first case, assume that the estimate is above the interval ($\hat{\theta} \ge \bar{\theta}+\kappa$).

As $\bar{\theta}+\kappa \ge \theta$ and $\tilde{g}(\theta,\tilde{\theta},u)$ is monotonically increasing in $\tilde{\theta}$, equation 9 can be converted to the differential inequality

$$\dot{\hat{\theta}}(t) \le -k\tilde{g}(\theta(t-\Delta t),\hat{\theta}(t)-(\bar{\theta}+\kappa),u(t-\Delta t)) \quad (10)$$

From Property (1) we get

$$\dot{\hat{\theta}}(t) \le -k\gamma(\hat{\theta}(t)-(\bar{\theta}+\kappa)) \Leftrightarrow \quad (11)$$

$$\dot{\hat{\theta}}(t) - (\bar{\theta}+\kappa) \le -k\gamma\hat{\theta}(t) \quad (12)$$

According to the Comparison Principle as seen in [35], the solution to the differential inequality (12) is bounded by the solution to the corresponding differential equation, thus

$$\hat{\theta}(t) - (\bar{\theta}+\kappa) \le \left(\hat{\theta}(0)-(\bar{\theta}+\kappa)\right)e^{-k\gamma t} \Leftrightarrow \quad (13)$$

$$\hat{\theta}(t) - \bar{\theta} \leq \kappa + \left(\hat{\theta}(0) - \bar{\theta} - \kappa\right) e^{-k\gamma t} \tag{14}$$

As $\hat{\theta} \geq \bar{\theta}$ we get

$$\left|\hat{\theta}(t) - \bar{\theta}\right| \leq \kappa + \left(\left|\hat{\theta}(0) - \bar{\theta}\right| - \kappa\right) e^{-k\gamma t} \tag{15}$$

which proves (6) for the first case.

ii) In the second case, assume that the estimate is below the interval ($\hat{\theta} \leq \bar{\theta} - \kappa$).

As $\bar{\theta} - \kappa \leq \theta$ and $\tilde{g}(\theta, \tilde{\theta}, u)$ has positive sensitivity to $\tilde{\theta}$, equation 9 can also be converted to the differential inequality

$$\dot{\hat{\theta}}(t) \geq -k\tilde{g}(\theta(t - \Delta t), \hat{\theta}(t) - (\bar{\theta} - \kappa), u(t - \Delta t)) \tag{16}$$

From Property (1) we get

$$\dot{\hat{\theta}}(t) \geq -k\gamma(\hat{\theta}(t) - (\bar{\theta} - \kappa)) \Leftrightarrow \tag{17}$$

$$\dot{\hat{\theta}}(t) - (\bar{\theta} - \kappa) \geq -k\gamma\hat{\theta}(t) \tag{18}$$

Application of the Comparison Principle again leads to

$$\hat{\theta}(t) - (\bar{\theta} - \kappa) \geq \left(\hat{\theta}(0) - (\bar{\theta} - \kappa)\right) e^{-k\gamma t} \Leftrightarrow \tag{19}$$

$$\hat{\theta}(t) - \bar{\theta} \geq -\kappa + \left(\hat{\theta}(0) - \bar{\theta} + \kappa\right) e^{-k\gamma t} \tag{20}$$

Since $\hat{\theta} \leq \bar{\theta}$ we get

$$\left|\hat{\theta}(t) - \bar{\theta}\right| \leq \kappa + \left(\left|\hat{\theta}(0) - \bar{\theta}\right| - \kappa\right) e^{-k\gamma t} \tag{21}$$

which proves (6) for the second case.

iii) The third and last case where the estimate is inside the interval obviously also fulfills (6). ∎

As $|\theta(t) - \bar{\theta}| \leq \kappa$, a consequence of Theorem 1 is that the absolute value of the parameter estimation error will converge toward 2κ or less without overshoot and with a minimum convergence rate of $k\gamma$.

Definition 2: A joint state and parameter observer for the system defined by (4) is

$$\dot{\hat{x}} = \frac{1}{\tau}\left(g(\hat{\theta}(t), u(t)) - \hat{x}\right) \tag{22a}$$

$$\hat{\theta}(t) = k \cdot \left(\tau y(t) + \int y(t) - g(\hat{\theta}(t), u(t - \Delta t))\,\mathrm{dt}\right) \tag{22b}$$

where $k > 0$.

Theorem 2: Let the observer defined by (22) be used for observing the state x and the parameter θ of the system defined by (4). If Property 1 is fulfilled, then $\tilde{x}$ is bounded by (29).

Proof of Theorem 2: The differential equation of the state estimate error is

$$\tau\dot{\tilde{x}} = \tau\dot{\hat{x}} - \tau\dot{x} = -\hat{x} + g(\hat{\theta}(t), u(t)) + x - g(\theta, u(t)) \Leftrightarrow \tag{23}$$

$$\tau\dot{\tilde{x}} = -\tilde{x} + \tilde{g}(\theta(t), \tilde{\theta}(t), u(t)) \tag{24}$$

From Property 1 we get

$$-\rho\left|\hat{\theta}(t) - \theta\right| \leq \tilde{g}(\theta(t), \tilde{\theta}(t), u(t)) \leq \rho\left|\hat{\theta}(t) - \theta\right| \tag{25}$$

Furthermore, from Theorem 1,

$$\left|\hat{\theta}(t) - \theta\right| \leq \left|\hat{\theta}(t) - \bar{\theta}\right| + \kappa \leq 2\kappa + \left(\left|\hat{\theta}(0) - \bar{\theta}\right| - \kappa\right) e^{-k\gamma t} \tag{26}$$

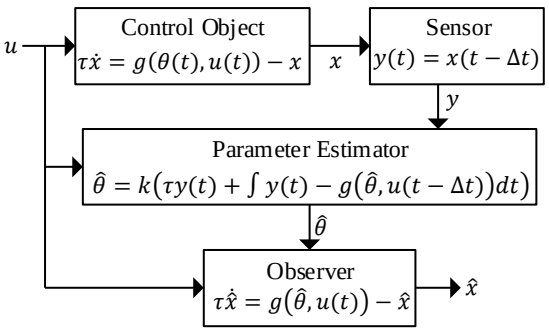

Fig. 2. Overview of the signal paths of the joint parameter and state observer. The parameter estimator uses the inputs and the sensor signal, whereas the observer only uses inputs and estimated parameter.

Combining (25) with (26) leads to two differential inequalities

$$\tilde{g}(\theta(t), \tilde{\theta}(t), u(t)) \geq -\rho\left(2\kappa + \left(\left|\hat{\theta}(0) - \bar{\theta}\right| - \kappa\right) e^{-k\gamma t}\right) \tag{27a}$$

$$\tilde{g}(\theta(t), \tilde{\theta}(t), u(t)) \leq \rho\left(2\kappa + \left(\left|\hat{\theta}(0) - \bar{\theta}\right| - \kappa\right) e^{-k\gamma t}\right) \tag{27b}$$

Inserting these into (24)

$$\tau\dot{\tilde{x}} \geq -\tilde{x} - \rho\left(2\kappa + \left(\left|\hat{\theta}(0) - \bar{\theta}\right| - \kappa\right) e^{-k\gamma t}\right) \tag{28a}$$

$$\tau\dot{\tilde{x}} \leq -\tilde{x} + \rho\left(2\kappa + \left(\left|\hat{\theta}(0) - \bar{\theta}\right| - \kappa\right) e^{-k\gamma t}\right) \tag{28b}$$

Using the Comparison Principle once again allows us to solve the differential inequalities

$$\tilde{x}(t) \geq -2\rho\kappa + (\tilde{x}(0) + 2\rho\kappa)\, e^{-\frac{t}{\tau}} - \eta\left(e^{-k\gamma t} - e^{-\frac{t}{\tau}}\right) \tag{29a}$$

$$\tilde{x}(t) \leq 2\rho\kappa + (\tilde{x}(0) - 2\rho\kappa)\, e^{-\frac{t}{\tau}} + \eta\left(e^{-k\gamma t} - e^{-\frac{t}{\tau}}\right) \tag{29b}$$

where

$$\eta = \frac{\rho\left(\left|\hat{\theta}(0) - \bar{\theta}\right| - \kappa\right)}{1 - k\gamma\tau} \tag{30}$$

Thus $|\tilde{x}(t)|$ will converge to $2\rho\kappa$ or lower with a minimum exponential convergence rate λ equal to the rate of the slowest converging term. Therefore $\lambda = \min(k\gamma\,,\, \frac{1}{\tau})$. ∎

Figure 2 shows an overview of the signal paths when combining control object and sensor with the joint state and parameter observer.

Note that the observer also can be applied to systems where the input nonlinearity has negative sensitivity to parameter estimation errors, opposite to what is specified in Property 1. This is achieved by inverting the sign of the parameter estimator equation. Consider as an example a system on the form (4) with

$$g(\theta, u) = -\theta \cdot (u^2 + 1) \tag{31}$$

The nonlinearity can be rewritten by defining $\psi = -\theta$ to

$$g_\psi(\psi, u) = \psi \cdot (u^2 + 1) \tag{32}$$

Now $g_\psi()$ fulfills Property 1 and ψ can be estimated according to Definition 1

$$\hat{\psi}(t) = k \cdot \left(\tau y(t) + \int_0^t y(t) - g_\psi(\hat{\psi}(t), u(t - \Delta t))\,\mathrm{dt}\right) \tag{33}$$

As $g_\psi(\psi, u) = g(\theta, u)$ we get

$$\hat{\theta}(t) = -k \cdot \left(\tau y(t) + \int_0^t y(t) - g(\hat{\theta}(t), u(t-\Delta t))\,\mathrm{dt} \right) \quad (34)$$

Thus for systems with negative sensitivity to parameter errors the sign of the parameter estimator should be switched.

The choice of observer gain k depends on the application. A high gain leads to fast convergence but also challenges the observer with regards to robustness to model inaccuracy and noise. As the observer has a direct gain from measurement to parameter estimate the observer might not be suited for control objects with significant sensor noise.

Note that when $\theta(t)$ is constant, $\kappa = 0$ and the observer errors converge exponentially to zero.

V. Comparison

The strength of the design presented here is the simplicity of the estimator for the case of the MISO Hammerstein system. This is in contrast to the design presented by [6] that solves the parameter estimation problem for a wider class of systems with a more complex estimator. For comparison, the design presented by [6] is applied to the problem solved by the parameter estimator from Definition 1. That is, estimating the parameter θ of the system (4). The resulting parameter estimator is[2]

$$\dot{z} = -k_\phi \left(\hat{\phi} - \frac{1}{\tau} y(t) \right) - \frac{1}{\tau} \frac{\partial g}{\partial \theta}(\hat{\theta}, u(t-\Delta t)) \cdot k_\theta \left(\tau \hat{\phi} - g(\hat{\theta}, u(t-\Delta t)) \right) \quad (35)$$

$$\hat{\phi} = z + k_\phi \frac{y(t)}{\tau} + \frac{1}{\tau} g(\hat{\theta}, u(t-\Delta t)) \quad (36)$$

$$\dot{\hat{\theta}} = k_\theta \left(\tau \hat{\phi} - g(\hat{\theta}, u(t-\Delta t)) \right) \quad (37)$$

The difference in complexity is clear when comparing to Definition 1. The estimator from [6] requires online calculation of $\frac{\partial g}{\partial \theta}$, an additional internal state z and an additional tuning parameter. An exponentially converging upper bound of $|\tilde{\theta}|$ was derived in [6], but it depends on the selection of a Lyapunov function and does not rule out the possibility of overshoot.

VI. Simulation Example

This section demonstrates the efficacy of the observer with a simple simulated example. The nonlinear part, $g(\theta, u)$, of the system is defined as

$$g(\theta, u) = \theta \cdot (u^2 + 1) \quad (38)$$

Taking the partial derivative with respect to θ leads to

$$\frac{\partial g(\theta, u)}{\partial \theta} = u^2 + 1 \quad (39)$$

For $|u(t)| \leq 2$ the system fulfills Property 1 with $\gamma = 1$ and $\rho = 5$. Theorem 2 facilitates the design of a joint state and parameter observer with errors that converge exponentially.

[2]Design choice for $\dot{\hat{\theta}}$ is based on (9).

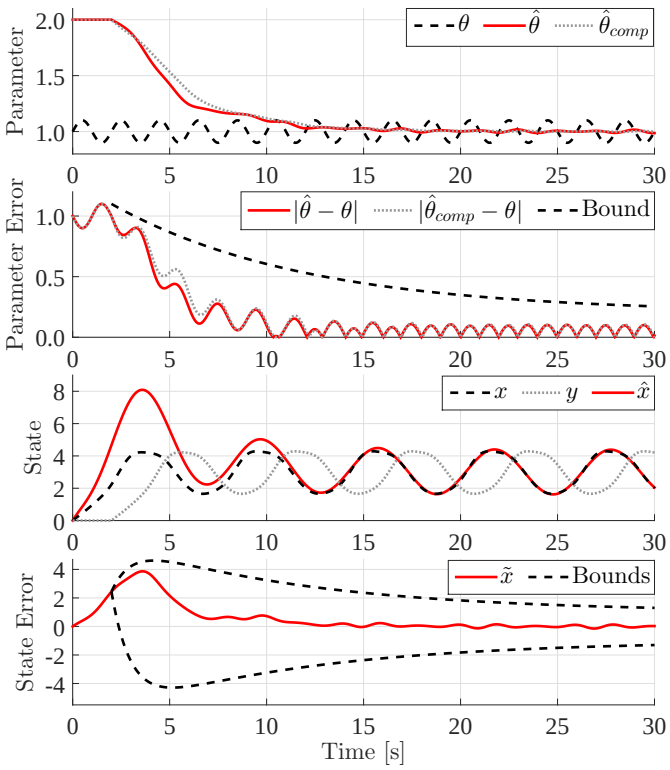

Fig. 3. Simulation of the observer applied to a simple system. The errors converge within the bounds and the state estimate is not delayed like the measurement. The observer performance is similar to that of the more complex parameter estimator ($\hat{\theta}_{comp}$) from Section V.

The system and the observer are simulated with $\tau = 1$ s, $\Delta t = 2$ s, $k = 0.1$, $\theta = 1$, $u(t) = 2\sin(\frac{\pi t}{6})$ and , $\theta(t) = 1 + 0.1\sin(\pi t)$, thus $\bar{\theta} = 1$ and $\kappa = 0.1$. The simulated observer errors are shown in Figure 3 along with the calculated bounds. The parameter estimate starts updating after 2 seconds as it needs a recording of the input signals with a length equal to the delay. The bottom plot compares the state to the measurement and the estimate. Figure 3 also shows the performance of the parameter estimator ($\hat{\theta}_{comp}$) from Section V simulated with similar gains. There is no significant performance difference between the two parameter estimates in this example.

VII. Adaptive Observer for Oxygen Estimation

The joint state and parameter observer is applied to the EGR system by defining state, measurement and inputs as, respectively

$$x = O_{sr}\ ,\ y = O_{srm}\ ,\ u = \begin{bmatrix} \dot{n}_f & \dot{n}_{egr} & \omega_{tc} \end{bmatrix}^T \quad (40)$$

and the input nonlinearity of the Hammerstein model as

$$g(\theta, u) = O_a - \frac{(1 + \frac{y}{4}(O_a + 1))\dot{n}_f \dot{n}_{egr}}{(\theta\beta(\omega_{tc}) + \frac{y}{4}\dot{n}_f)(\theta\beta(\omega_{tc}) + \dot{n}_{egr})} \quad (41)$$

The values of ρ and γ are found as the limits to

$$\frac{\partial g}{\partial \theta} = \left(1 + \frac{y}{4}(O_a + 1)\right) \frac{\dot{n}_f \dot{n}_{egr} \beta \left(2\beta + \frac{y}{4}\dot{n}_f + \dot{n}_{egr}\right)}{\left(\theta\beta + \frac{y}{4}\dot{n}_f\right)^2 (\theta\beta + \dot{n}_{egr})^2} \quad (42)$$

These limits depend on the possible combinations of inputs which are difficult to determine. Conservative values can be

calculated by defining independent intervals for the inputs. For a typical engine this approach results in limits of the order $\rho = 10^{-3}$, $\gamma = 10^{-5}$. With an estimator gain of 100 (as used in the experiments) this leads to a convergence bound with a time constant of 15 minutes. This is considered as a theoretical result that guarantees convergence in worst-case rather than an indicator of expected performance, as all simulations and experiments show much faster convergence. A combination of inputs that results in $\gamma = 10^{-5}$ (and thus slow convergence) only exists for short intervals as the inputs to the COM are not independent in the physical system.

The following sections show the observer applied to EGR systems with increasing levels of realism. As the observer has more than enough time for initial convergence during the fixed-input EGR startup phase, our main focus is engine loading transients where the observer has to be robust against model inaccuracy and variations of θ.

A. Results from control-oriented model

The joint state and parameter observer is first applied to a simulation of the control-oriented EGR model. The scenario is an engine loading transient with subsequent adjustment of turbocharger speed and EGR flow. The value of θ is changed in a step, to illustrate the convergence bounds. Figure 4 shows the results. $\theta(t)$ is constant after the step at 50 seconds, so the observer errors converge to zero. The convergence bound for this period is shown in Figure 4. With respect to the oxygen fraction, the observer is able to produce a reasonable instantaneous estimate of the simulated state during the loading transient in spite of the change of θ.

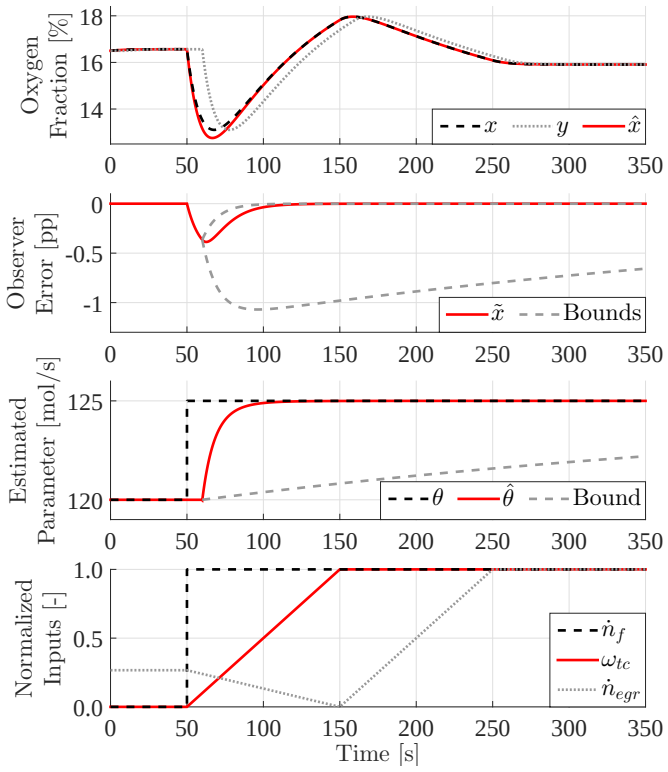

Fig. 4. Results from application of the joint state and parameter observer to a simulation of the control-oriented EGR model.

B. Results from high-fidelity simulation

The observer is now applied to a simulation of the high-fidelity model of the full air path of a marine diesel engine with high pressure EGR presented in [32]. This model includes more complex dynamics than the COM and thus challenges the observer robustness. As before the scenario is a load transient, but in this case θ, the turbocharger speed and the EGR flow are simulated by the model. The EGR blower speed is adjusted after the transient. Figure 5 shows the results. The transition through the operating region makes the simulated θ change. The parameter estimate fluctuates slightly during the first part of the transient and travels outside the interval to which $\theta(t)$ belongs. This is due to the small differences in dynamics between the COM and the high-fidelity model which are not accounted for in the convergence proofs. As before the observer is able to estimate the oxygen fraction without delay and with reasonable accuracy during the transient.

The high-fidelity model depends on turbine and compressor maps for flow calculation. These maps only cover pressure conditions present in the upper half of the engine load region. Research into extrapolation of the model to low load conditions is still ongoing. Most of the problematic loading transients occur in the lower half where auxiliary blowers aid the turbocharger compressor in maintaining scavenge pressure. The validity of the joint state and parameter observer in the low load region is tested experimentally.

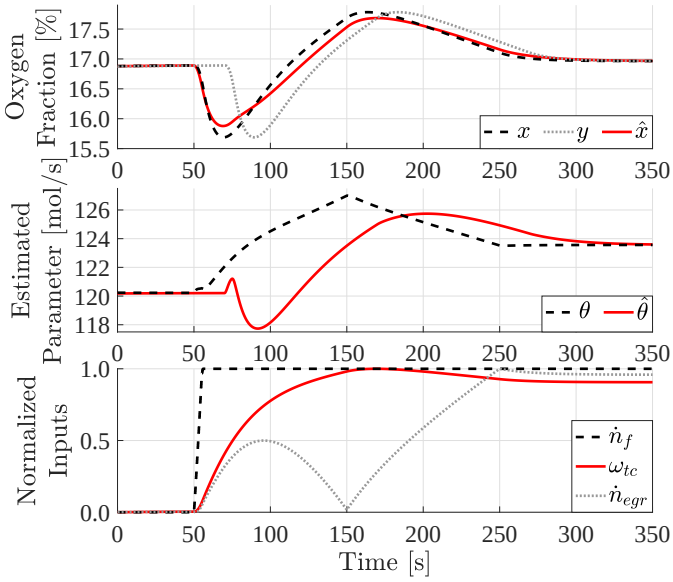

Fig. 5. Results from application of the joint state and parameter observer to a simulation of a high-fidelity model of a diesel engine airpath.

C. Results from engine test bed

The observer is experimentally validated by applying it to data recorded from an engine test bed, in this case the 4T50ME-X large two-stroke engine situated in engine designer MAN Diesel & Turbo's Diesel Research Center in Copenhagen. Figure 6 shows the result of applying the observer to a load ramp in the lower half of the load range. In this region θ is higher as the auxiliary blowers increase the flow. Small

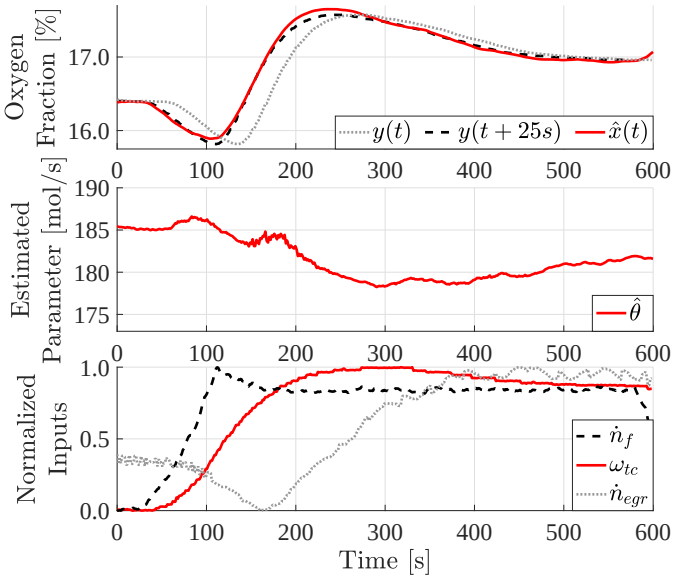

Fig. 6. Results from application of the joint state and parameter observer to an engine load ramp performed on an engine test bed.

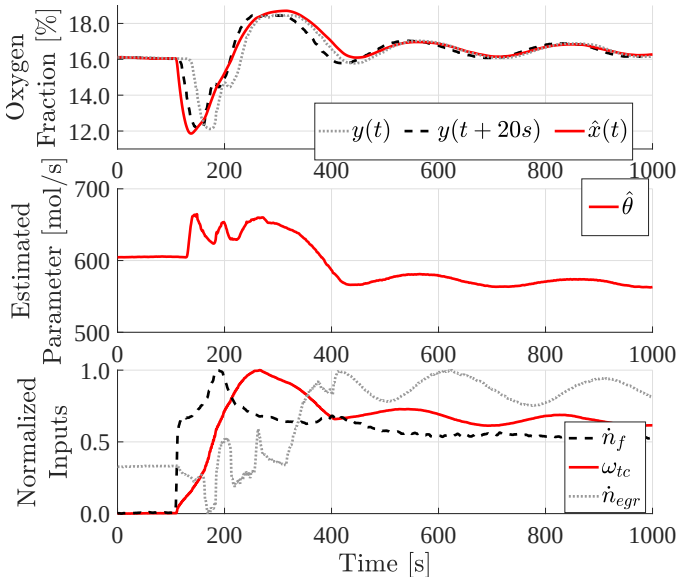

Fig. 7. Results from application of the joint state and parameter observer to an engine speed setpoint step performed on a vessel operating at sea.

fluctuations occur in the parameter estimate, but the observer is able to predict the measurement with reasonable accuracy in spite of the auxiliary blowers.

D. Results from vessel

The final validation is carried out by applying the observer to an example of the unfortunate scenario that it is meant to alleviate. The dataset in question stems from the 4500 TEU container vessel Maersk Cardiff, operating in the South China Sea. When moving at steady state at approximately 10% engine load, the bridge performed an engine speed setpoint step. Engine load peaked at 43% during the transient and stabilized at about 27%. The slow response of the EGR controller led to a severe drop in O_{sr} from 16% to 12% with subsequent oscillations. This drop resulted in formation of thick black exhaust smoke for more than 45 seconds.

Results from application of the observer is shown in Figure 7. The vessel engine is approximately 3 times larger than the test bed engine, and θ scales similarly. The observer is challenged by the extreme scenario and the input transients, especially in EGR flow, propagates to $\hat{\theta}$. It is difficult to determine whether the fluctuating behavior of $\hat{\theta}$ is due to model inaccuracy or whether it represents actual transient behavior of $\theta(t)$. In any case, the state observer is able to predict the O_{sr} drop 20 seconds before the sensor, with acceptable accuracy. The EGR controller would benefit significantly from this information in order to decrease the EGR flow during the transient and thus avoid unacceptable smoke formation.

VIII. Conclusions

Designs for both a *parameter estimator* and a *joint state and parameter observer* were presented along with derivation of exponentially converging bounds on state and parameter errors. A simulation example illustrated the performance of the resulting observer and it the complexity was favorably compared to the method of [7]. It was shown that while the suggested approach applies to a more narrow class of systems, the present design is simpler and provides better knowledge about error behavior. Application of the observer to a high-pressure exhaust gas recirculation system for large two-stroke diesel engines at test bed and at sea showed that the suggested method is a promising candidate to become enabling technology for estimator-based control of exhaust gas recirculation, and thereby a cornerstone in order for large marine diesel engines to meet strict emission requirements in NO_x and soot formation.

If the proposed method is used in contexts where bounded but unknown disturbances are present, an assessment needs to be made of the effects of unknown disturbances on the quality of the estimates.

Acknowledgment

This work was partially funded by the Danish Agency for Science, Technology and Innovation, under grant number 1355-00071B.

References

[1] G. Besançon, *Nonlinear observers and applications*. Springer Berlin Heidelbarg, 2007.
[2] Ljung, "Asymptotic behavior of the extended kalman filter as a parameter estimator for linear systems," *IEEE Transac. on Automatic Control*, vol. 24, no. 1, pp. 36–50, 1979.
[3] W. Zhou and M. Blanke, "Identification of a class of nonlinear state space models using rpe techniques," *IEEE Transac. on Automatic Control*, vol. 34, pp. 312–316, 1989.
[4] J.-J. Slotine and W. Li, *Applied nonlinear control*. Prentice-Hall, 1991.
[5] A. Annaswamy, F. Skantze, and A. Lohi, "Adaptive control of continuous time systems with convex/concave parametrization," *Automatica*, vol. 34, no. 1, pp. 33–49, 1998.
[6] H. Grip, T. Johansen, L. Imsland, and G.-O. Kaasa, "Parameter estimation and compensation in systems with nonlinearly parameterized perturbations," *Automatica*, vol. 46, no. 1, pp. 19–28, 2010.
[7] H. Grip, A. Saberi, and T. Johansen, "Estimation of states and parameters for linear systems with nonlinearly parameterized perturbations," *Syst. and Control Letters*, vol. 60, no. 9, pp. 771–777, 2011.

[8] X. Liu, R. Ortega, H. Su, and J. Chu, "On adaptive control of nonlinearly parameterized nonlinear systems: Towards a constructive procedure," *Syst. and Control Letters*, vol. 60, no. 1, pp. 36–43, 2011.

[9] V. Adetola, M. Guay, and D. Lehrer, "Adaptive estimation for a class of nonlinearly parameterized dynamical systems," *IEEE Transac. on Automatic Control*, vol. 59, no. 10, pp. 2818–2824, 2014.

[10] I. Tyukin, E. Steur, H. Nijmeijer, and C. van Leeuwen, "Adaptive observers and parameter estimation for a class of systems nonlinear in the parameters," *Automatica*, vol. 49, no. 8, pp. 2409–2423, 2013.

[11] I. Tyukin, "Adaptation algorithms in finite form for nonlinear dynamic objects," *Automation and Remote Control*, vol. 64, no. 6, pp. 951–974, 2003.

[12] E. Eskinat, S. Johnson, and W. Luyben, "Use of hammerstein models in identification of nonlinear systems," *AIChE Journal*, vol. 37, no. 2, pp. 255–268, 1991.

[13] K. Narendra and P. Gallman, "An iterative method for the identification of nonlinear systems using a hammerstein model," *IEEE Transac. on Automatic Control*, vol. 11, no. 3, pp. 546–550, 1966.

[14] P. Mattsson and T. Wigren, "Convergence analysis for recursive hammerstein identification," *Automatica*, vol. 71, pp. 179–186, 2016.

[15] D. Laila and E. Gruenbacher, "Nonlinear output feedback and periodic disturbance attenuation for setpoint tracking of a combustion engine test bench," *Automatica*, vol. 64, pp. 29–36, 2016.

[16] P. Falugia, L. Giarre, and G. Zappa, "Approximation of the feasible parameter set in worst-case identification of hammerstein models," *Automatica*, vol. 41, no. 6, pp. 1017–1024, 2005.

[17] E. Bai, "Frequency domain identification of hammerstein models," *IEEE Transac. on Automatic Control*, vol. 48, no. 4, pp. 530–542, 2003.

[18] W.-X. Zhao and H.-F. Chen, "Adaptive tracking and recursive identification for hammerstein systems," *Automatica*, vol. 45, no. 12, pp. 2773–2783, 2009.

[19] S. Sastry, *Nonlinear systems: analysis, stability and control*. Springer, 1999.

[20] IMO, *Marpol ANNEX VI and NTC 2008, 2013: With guidelines for implementation*. International Maritime Organisation, 2013.

[21] HELCOM, "Workshop in russia advances neca for ships in baltic and north seas," http://www.helcom.fi/news/Pages/Workshop-in-Russia-advances-NECA-for-ships-in-Baltic-and-North-Seas.aspx, 2016.

[22] J. Heywood, *Internal combustion engine fundamentals*. McGraw-Hill, 1988.

[23] J. Wahlström and L. Eriksson, "Modelling diesel engines with a variable-geometry turbocharger and exhaust gas recirculation by optimization of model parameters for capturing non-linear system dynamics," *Proceedings of the Institution of Mechanical Engineers, Part D, Journal of Automobile Engineering*, vol. 225, no. 7, pp. 960–986, 2011.

[24] M. Jankovic, M. Jankovic, and I. Kolmanovsky, "Constructive lyapunov control design for turbocharged diesel engines," *IEEE Transactions On Control Systems Technology*, vol. 8, no. 2, pp. 288–299, 2000.

[25] J. Wahlström, L. Eriksson, and L. Nielsen, "Egr-vgt control and tuning for pumping work minimization and emission control," *IEEE Transactions on Control Systems Technology*, vol. 18, no. 4, pp. 993–1003, 2010.

[26] J. Wahlström and L. Eriksson, "Output selection and its implications for mpc of egr and vgt in diesel engines," *IEEE Transactions on Control Systems Technology*, vol. 21, no. 3, pp. 932–940, 2013.

[27] M. Huang, K. Zaseck, K. Butts, and I. Kolmanovsky, "Rate-based model predictive controller for diesel engine air path: Design and experimental evaluation," *IEEE Transactions on Control Systems Technology*, 2016.

[28] A. Stefanopoulou and R. Smith, "Maneuverability and smoke emission constraints in marine diesel propulsion," *Control Engineering Practice*, vol. 8, no. 9, pp. 1023–1031, 2000.

[29] J. Zhao and J. Wang, "Adaptive observer for joint estimation of oxygen fractions and blend level in biodiesel fueled engines," *IEEE Transactions on Control Systems Technology*, vol. 23, no. 1, pp. 80–90, 2015.

[30] J. Hansen, C. Zander, N. Pedersen, M. Blanke, and M. Vejlgaard-Laursen, "Modelling for control of exhaust gas recirculation on large diesel engines," *Proceedings of the 9th IFAC Conference on Control Applications in Marine Systems*, pp. 380–385, 2013.

[31] G. Alegret, X. Llamas, M. Vejlgaard-Laursen, and L. Eriksson, "Modeling of a large marine two-stroke diesel engine with cylinder bypass valve and egr system," *IFAC-PapersOnLine*, vol. 48, no. 16, pp. 273 – 278, 2015.

[32] K. Nielsen, M. Blanke, L. Eriksson, and M. Vejlgaard-Laursen, "Control-oriented model of molar scavenge oxygen fraction for exhaust recirculation in large diesel engines," *ASME Journal of Dynamic Systems, Measurement and Control*, vol. 139, no. 2, Feb. 2017.

[33] J. Hansen, M. Blanke, H. Niemann, and M. Vejlgaard-Laursen, "Exhaust gas recirculation control for large diesel engines - achievable performance with siso design," *Proceedings of the 9th IFAC Conference on Control Applications in Marine Systems*, pp. 346–351, 2013.

[34] K. Nielsen, M. Blanke, and M. Vejlgaard-Laursen, "Nonlinear adaptive control of exhaust gas recirculation for large diesel engines," *IFAC-PapersOnLine*, vol. 48, no. 16, pp. 254 – 260, 2015.

[35] H. Khalil, *Nonlinear systems*. Prentice Hall, 2002.